Farnesoid X receptor deletion improves cardiac function, structure and remodeling following myocardial infarction in mice

JIANSHU GAO[1,2*], XIAOQIANG LIU[3*], BINGJIAN WANG[4*], HAIYAN XU[4], QIANG XIA[5], TIANFEI LU[5] and FANG WANG[1]

[1]Department of Cardiology, Shanghai General Hospital of Nanjing Medical University, Shanghai 200080; [2]Department of Cardiology, Yancheng First People's Hospital, Nantong University, Yancheng, Jiangsu 224005; [3]Department of Cardiology, Shanghai General Hospital, Shanghai Jiao Tong University School of Medicine, Shanghai 200080; [4]Department of Cardiology, Huai'an First People's Hospital, Nanjing Medical University, Huai'an, Jiangsu 223300; [5]Department of Transplantation and Hepatic Surgery, Renji Hospital, Shanghai Jiao Tong University School of Medicine, Shanghai 200080, P.R. China

Abstract. The farnesoid X receptor (FXR) is implicated in cholesterol and bile acid homeostasis; however, its role following myocardial infarction (MI) has yet to be elucidated. The aim of the present study was to investigate the effects of FXR knockout on left ventricular (LV) remodeling following MI. Coronary arteries of wild type (WT) and FXR$^{-/-}$ mice were permanently occluded to cause MI, and serial echocardiographic and histological tests were conducted. At 4 weeks post-MI, FXR$^{-/-}$ mice exhibited significantly smaller infarct sizes (34.20±2.58 vs. 44.20±3.19%), improved ejection fraction (47.31±1.08 vs. 37.64±0.75%) and reduced LV chamber dilation compared with WT mice. LV remodeling was significant as early as 7 days post-MI in FXR$^{-/-}$ compared with WT mice. Histological features associated with enhanced long-term remodeling and improved functionality, such as increased angiogenesis via detection of CD31 and reduced fibrosis, were observed in the FXR$^{-/-}$ group. Myocyte apoptosis within the infarcted zones appeared significantly reduced by day 7 in FXR$^{-/-}$ mice. In conclusion, the results of the present study suggested that FXR knockout may participate in the preservation of post-MI cardiac functionality, via reducing fibrosis and chronic apoptosis, and ameliorating ventricular function.

Correspondence to: Dr Fang Wang, Department of Cardiology, Shanghai General Hospital of Nanjing Medical University, 650 Songjiang Road, Shanghai 200080, P.R. China
E-mail: wangfang150505@163.com

Dr Tianfei Lu, Department of Transplantation and Hepatic Surgery, Renji Hospital, Shanghai Jiao Tong University School of Medicine, 1630 Dongfang Road, Shanghai 200080, P.R. China
E-mail: lutianfei@medmail.com.cn

*Contributed equally

Introduction

Myocardial infarction (MI) is a leading cause of congestive heart failure. The left ventricle (LV) undergoes molecular, cellular and extracellular matrix alterations following MI that can significantly affect myocardial size, shape and function (1). Ventricular remodeling due to persistent hypoxia and ischemia following MI has been associated with the development of heart failure (2). Therefore, elucidating the mechanisms underlying post-MI ventricular remodeling may yield novel therapeutic targets for the treatment of patients with cardiac disorders.

The nuclear hormone receptor family comprises of transcriptional regulators that have been implicated in numerous physiological and pathophysiological functions, such as cellular metabolism, proliferation and apoptosis, as well as tumorigenesis and angiogenesis. Several nuclear hormone receptors, such as liver X receptors α and β, and the estrogen, androgen and retinoic acid receptors, have been implicated in the physiological regulation of cardiovascular function (3-8). The farnesoid X receptor (FXR; NR1H4) is another member of the nuclear receptor superfamily (9-12). FXR expression is localized primarily in the liver, intestine, kidneys and adrenal glands, where it regulates the homeostasis and metabolism of cholesterol, bile acid and lipids (9). FXR is also expressed in the heart and adipose tissue, and in the vasculature (11,13,14). Previous studies have suggested that FXR, apart from its implication in metabolism, may serve an important role in cardiovascular physiology and pathology (15,16). FXR has been identified as a novel apoptotic mediator and has been revealed to contribute to myocardial ischemia/reperfusion injury (13). However, the mechanisms underlying the implication of FXR in pathophysiological processes following MI have yet to be elucidated. Therefore, the aim of the present study was to investigate the effects of FXR knockdown on LV remodeling and dysfunction following MI.

Materials and methods

Ethics statement. The present study was conducted according to the Guide for the Care and Use of Laboratory Animals

published by the US National Institutes of Health (NIH Publication No. 85-23, revised 1996) and was approved by the Ethics Review Board for Animal Studies of Shanghai Jiaotong University School of Medicine (approval no. SYKX-2008-0050; Shanghai, China).

Animals. FXR$^{-/-}$ and wild type (WT) male mice were obtained from The Jackson Laboratory (Bar Harbor, ME, USA). FXR$^{-/-}$ mice and control WT C57BL/6 mice (age, 8-12 weeks; weight, 20-25 g) were housed in a specific pathogen-free barrier facility at 24˚C, 55% humidity and under 12/12 h light/dark cycles, with free access to food and water.

Mouse model of MI. The MI model was generated by an experienced investigator who was blind to the experiment. Mice were anesthetized with 2% isoflurane prior to treatment with 0.5% bupivacaine. The left anterior descending coronary artery (LAD) was ligated as previously described (17). Sham-operated mice (n=6) underwent open chest surgery without coronary artery ligation. A total of 6 WT and 6 FXR$^{-/-}$ mice that underwent MI (n=6) were sacrificed on days 7 and 28 following MI. All possible measures were taken to minimize suffering.

Ultrasonic echocardiography (UCG) assessment. Cardiac function was evaluated using transthoracic UCG prior to surgery and 1 day, 1 week and 4 weeks following MI in a blind manner. UCG was performed using the Vevo® 2100 ultrasound system (VisualSonics, Inc., Toronto, ON, Canada) equipped with a 30 MHz transducer.

LV dimensions were examined digitally in M-mode tracings and averaged from three consecutive cardiac cycles. LV end-systolic diameter (LVESD) and end-diastolic diameter (LVEDD), interventricular septal thickness in diastole and LV posterior wall thickness were assessed. The percentage of LV fractional shortening (%FS) was calculated as follows: % FS = (LVEDD-LVESD)/LVEDD x 100 (%).

Assessment of infarct size. 2,3,5-triphenyltetrazolium chloride (TTC) was used for assessment of the infarction size. Briefly, 28 days after surgery the hearts from randomly selected mice were removed, frozen at -20˚C and cut into 1-mm thick sections perpendicular to the long axis of the heart. The hearts of these mice were harvested to assess the infarct size only. It was observed that the infarct area was not stained, and the non-infarct area was dyed red. The slice was photographed with a digital camera following TTC staining. Infarct size on day 28 post-MI was evaluated, as described by Pfeffer *et al* (18,19), and calculated as a percentage of the whole LV size, using ImageJ version k1.45 software (National Institutes of Health, Bethesda, MD, USA).

Histological examination. The hearts of left ventricular myocardium were arrested by intravenous administration of 2 mol/l KCl (Shanghai Pharmaceuticals Holding Co., Ltd., Shanghai, China) following isoflurane anesthesia and abdominal aorta bleeding. The samples were immediately fixed with 4% paraformaldehyde at room temperature for 24 h and dehydrated, paraffin embedded and sliced into 4 μm sections, on weeks 1 and 4 following MI, to be used for terminal deoxynucleotidyl transferase dUTP nick-end labeling (TUNEL) assay,

hematoxylin and eosin (H&E) staining, Masson's trichrome staining for interstitial fibrosis and α-smooth muscle actin (α-SMA) staining. Paraffin-embedded tissue sections were stained with a Masson's trichrome Staining kit (cat. no. G1006; Wuhan Goodbio Technology Co.,Ltd.,Wuhan,China).Collagen volume fraction (CVF) was quantified and calculated as an area of Masson's trichrome-stained connective tissue divided by total area of the image as previously described (17,18) using Image Pro Plus software (Media Cybernetics, Inc., Rockville, MD, USA). Immunohistochemical staining of α-SMA as a marker of myocardial fibrosis after myocardial infarction was also performed. Paraffin-embedded tissue sections were stained with an α-SMA primary antibody (1:2,000; cat. no. GB13063; Wuhan Goodbio Technology Co., Ltd., Wuhan, China) overnight at 4˚C, washed three times with PBS and incubated with HRP-conjugated secondary goat anti mouse IgG (1:10,000; cat. no. K5007; Wuhan Goodbio Technology Co., Ltd., Wuhan, China) for 50 min at room temperature. Samples were counterstained with hematoxylin and incubated at room temperature for 3 min. Stained sections were observed under a confocal laser scanning microscope. LV diameter was measured in two perpendicular axes and averaged for each animal (18). LVEDD was measured as previously described (19). Myocyte size was measured using cross sections midway between the base and apex of the LV with hematoxylin and eosin (H&E) staining.

Western blot analysis. FXR$^{-/-}$ and WT C57BL/6 mice were sacrificed on days 3, 7 and 28 post-MI for the collection of heart samples. Proteins extracted from heart tissue were analyzed using western blot analysis. The harvested ventricular tissue was homogenized and lysed using lysis buffer containing 1 protease inhibitor cocktail tablet per 10 ml of lysis reagents (Roche Diagnostics, Indianapolis, IN, USA). Protein concentration was determined with a bicinchoninic acid (BCA) protein assay kit (Beyotime Institute of Biotechnology, Shanghai, China). For western blot analysis an equal amount of protein (60 mg) was loaded in each well and subjected to 12% sodium dodecyl-sulfate polyacrylamide gel electrophoresis. Separated proteins were then transferred from the gel to nitrocellulose membranes (Whatman; GE Healthcare Life Sciences, Chalfont, UK) and blocked with LI-COR blocking buffer for 1-2 h. The following primary antibodies were used: Anti-FXR (1:1,000; cat. no. 12295; Cell Signaling Technology, Inc., Danvers, MA, USA), anti-caspase 3 (1:800; cat. no. 9664; Cell Signaling Technology, Inc.) and anti-GAPDH (1:1,000; cat. no. 2118; Bioworld Technology, Inc., St. Louis Park, MN, USA). The secondary antibodies of HRP-conjugated goat anti mouse IgG (1:10,000; cat. no. 22855) were obtained from LI-COR Biosciences (Lincoln, NE, USA). The protein bands were visualized using an Odyssey infrared imaging system (LI-COR Biosciences). Protein levels were semi-quantified on duplicate blots with standard densitometry using Odyssey software version 3.0 (LI-COR Biosciences). The intensities of protein bands were normalized to those of GAPDH and expressed as fold increase relative to control.

Reverse transcription-quantitative polymerase chain reaction (RT-qPCR). As previously described (20,21), total RNA from tissues and cardiomyocytes was extracted using TRIzol®

Table I. Ultrasonic echocardiography performance 1 week following MI surgery.

Variable	WT sham	FXR$^{-/-}$ sham	WT MI	FXR$^{-/-}$ MI
n	6	7	8	8
EF%	68.32±1.05[a]	65.28±2.52	44.41±1.54[c]	47.63±1.42[b]
FS%	38.29±0.46[a]	39.18±0.53	21.57±1.23[c]	26.08±1.46[b]
LVEDD (mm)	3.47±0.10[a]	3.38±0.09	4.05±0.13[c]	3.85±0.12[b]
LVESD (mm)	2.17±0.11[a]	2.28±0.13	3.13±0.16[c]	2.85±0.15[b]

[a]P<0.05 vs. WT MI group; [b]P<0.05 vs. FXR$^{-/-}$ sham group. [c]P<0.05 vs. FXR$^{-/-}$ MI group. WT, wild type; MI, myocardial infarction; FXR, farnesoid X receptor; EF, ejection fraction; FS, fractional shortening; LVEDD, LV end-diastolic diameter; LVESD, LV end-systolic diameter; LV, left ventricular. Data are expressed as the mean ± standard error of the mean.

Table II. Ultrasonic echocardiography performance 4 weeks following MI surgery.

Variable	WT sham	FXR$^{-/-}$ sham	WT MI	FXR$^{-/-}$ MI
n	9	9	10	10
EF%	72.13±0.86[a]	70.35±1.13	37.64±0.77	47.31±1.08[b]
FS%	37.25±0.63[a]	38.23±0.76	20.63±0.71	25.96±0.62[b]
LVEDD (mm)	3.45±0.12[a]	3.67±0.11	4.78±0.22	3.84±0.13[b]
LVESD (mm)	2.09±0.12[a]	2.21±0.10	3.99±0.12	3.10±0.10[b]

[a]P<0.05 vs. WT MI group. [b]P<0.05 vs. WT MI group. WT, wild type; MI, myocardial infarction; FXR, farnesoid X receptor; EF, ejection fraction; FS, fractional shortening; LVEDD, LV end-diastolic diameter; LVESD, LV end-systolic diameter; LV, left-ventricular. Data are expressed as the mean ± standard error of the mean.

Reagent (Invitrogen; Thermo Fisher Scientific, Inc., Waltham, MA, USA) according to the manufacturer's protocol. RNA was reverse transcribed into cDNA using M-MLV reverse transcriptase (Invitrogen; Thermo Fisher Scientific, Inc.). The following primers were used for qPCR: GAPDH, forward 5'-TCACTG CCACCCAGAAGA-3', reverse 5'-GACGGACACATTGGG GGTAG-3'; collagen III, forward 5'-GACCAAAAGGTGATG CTGGACAG-3', reverse 5'-CAAGACCTCGTGCTCCAG TTAG-3'; and matrix metalloproteinase (MMP)-9, forward 5'-GCTGACTACGATAAGGACGGCA-3' and reverse 5'-TAG TGGTGCAGGCAGAGTAGGA-3'. qPCR was performed on cDNA with a Real-Time PCR system (Bio-Rad Laboratories, Inc., Hercules, CA, USA), using SYBR Premix Ex Taq™ (Takara Bio, Inc., Otsu, Japan). The reactions of 10 μl volume contained 2X SYBR Premix Ex Taq™ (Takara Bio, Inc.) at 5 μl, each primer at 0.2 μl, and 0.2 μl of cDNA template (1:5 diluted) at 1 μl, RNase-free dH$_2$O at 3.6 μl. Amplification was performed under the following conditions: Initial denaturation step at 95˚C for 3 min, followed by 40 cycles of denaturation at 95˚C for 30 sec, annealing and extension at 60˚C for 30 sec. The relative expression levels for each gene were normalized to GAPDH and analyzed using the 2$^{-\Delta\Delta Cq}$ method (22).

TUNEL assay. Cellular apoptosis of left ventricular myocardium was assessed using the ApopTag® Fluorescein *In Situ* Apoptosis Detection kit (S7110; EMD Millipore, Billerica, MA, USA), according to the manufacturer's protocol. Cell nuclei were stained with 4'-6-diamidino-2-phenylindole
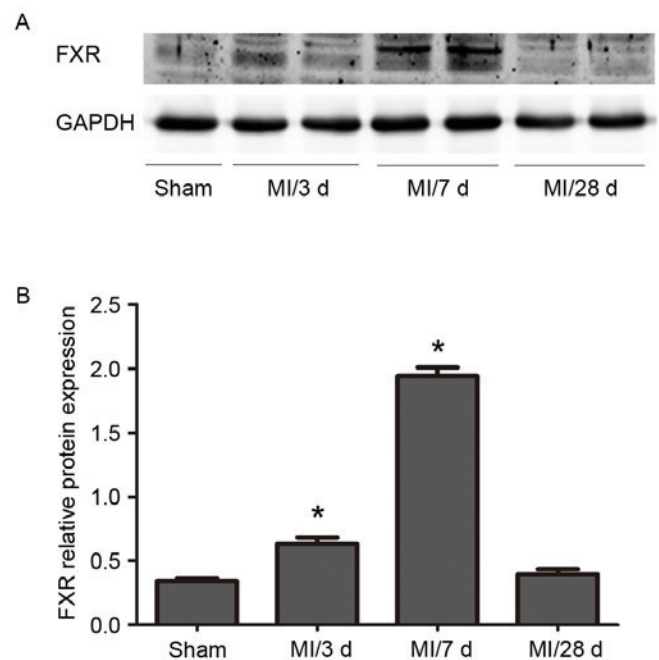

Figure 1. FXR expression in cardiac tissue. (A) FXR protein expression levels were assessed using western blot analysis. Tissue samples from infarct regions of WT mice that underwent MI and from corresponding regions of sham-operated WT mice were collected at various time points post-surgery (n=5/time point). (B) Western blot analysis results were semi-quantified and normalized to GAPDH. Data are expressed as the mean ± standard error of the mean. *P<0.05 vs. the sham group. FXR, farnesoid X receptor; WT, wild type; MI, myocardial infarction.

(DAPI), and incubated at room temperature for 10 min. Sections were mounted and observed under a FluoView™ FV1000 confocal microscope (Olympus Corporation, Tokyo, Japan). The number of TUNEL-positive cardiomyocyte nuclei was manually determined. At least 3 fields per section were analyzed, as previously described (23).

Immunofluorescence. Paraffin-embedded tissue sections were stained with an anti-cluster of differentiation (CD) 31 primary antibody (1:50; cat. no. GB13063; Wuhan Goodbio Technology Co., Ltd., Wuhan, China) overnight at 4˚C, washed three times with PBS and incubated with fluorescein isothiocyanate-conjugated secondary donkey anti-rabbit immunoglobulin G (1:200; cat. no. 705-165-003; Wuhan Goodbio Technology Co., Ltd.) for 1 h at room temperature in a darkened humidified chamber. Samples were counterstained with DAPI, and incubated at room temperature for 10 min. Stained sections were observed under a confocal laser scanning microscope using x200 and x400 magnifications.

Statistical analysis. The statistical significance of the difference between two groups was performed by unpaired Student's t test. The comparison of parameters among more than three groups was performed by one-way analysis of variance with Tukey's HSD post hoc test. Data are expressed as the mean ± standard error of the mean. The experiments were repeated 5 times. P<0.05 was considered to indicate a statistically significant difference. All analyses were performed using GraphPad Prism software version 5.0 (GraphPad Software, Inc., La Jolla, CA, USA).

Results

FXR protein expression levels in post-MI myocardial tissue. Western blot analysis revealed a progressive increase in FXR protein expression levels in WT mice between 3 days, 7 days and 28 days following LAD ligation. FXR levels declined at 28 days. (Fig. 1).

FXR^-/- mice demonstrate improved myocardial morphology and function post-MI. UCG was used to assess cardiac function 1 and 4 weeks post-MI (Tables I and II). %FS was used as a systolic function index and results indicated a significant improvement in FXR^-/- mice compared with in WT mice (Table II). Furthermore, FXR^-/- mice exhibited lower LVEDD and LVESD compared with WT mice (Fig. 2A). In addition, no significant difference in cardiac function was revealed between FXR^-/- and WT sham-operated mice (Tables I and II), suggesting that FXR knockout does not affect cardiac function under physiological conditions.

Infarct scar size appeared significantly reduced in the FXR^-/- compared with in the WT group (Fig. 2B and C). A 10% relative reduction in infarct size was reported in FXR^-/- mice compared with in WT mice. LV cavity size was preserved in the FXR^-/- group compared with in the WT group, as demonstrated by the significantly smaller LV diameters in FXR^-/- mice (Table II).

Microvesicular density and fibrosis. Masson's trichrome staining for interstitial fibrosis in the border zone is
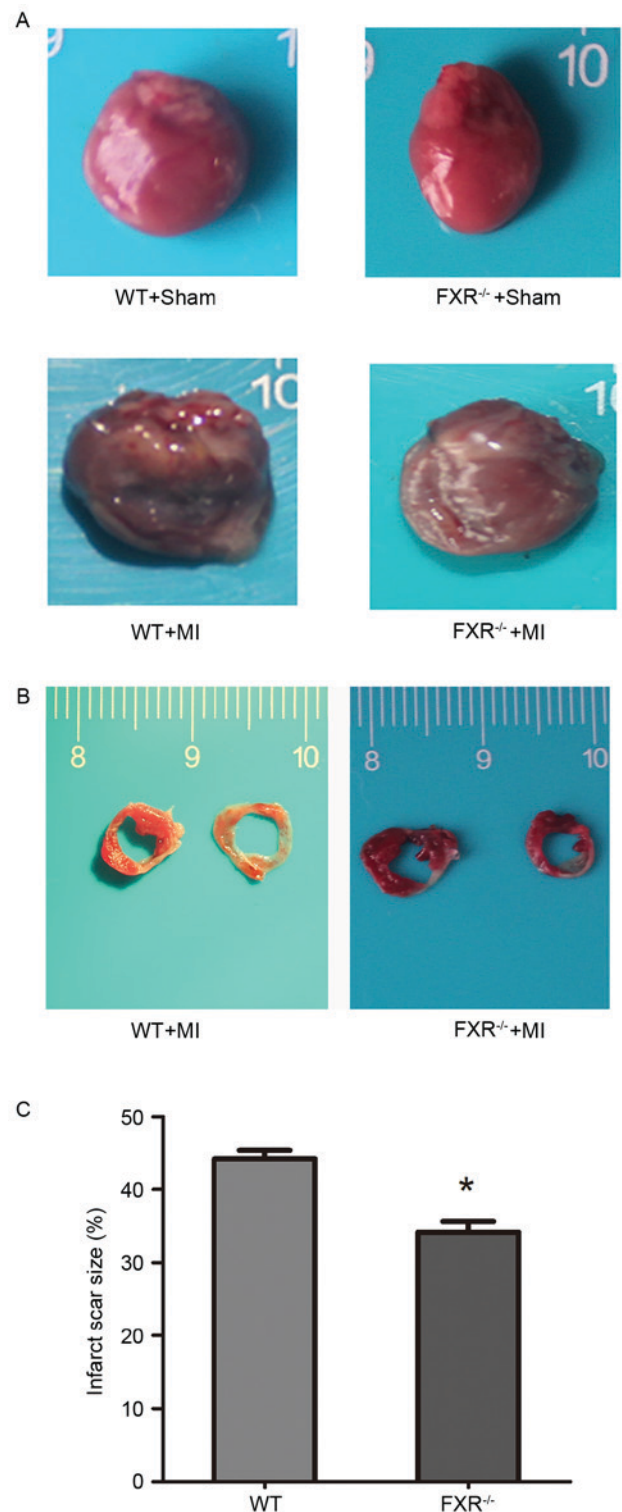

Figure 2. Cardiac structure and function in mice following MI. (A) Representative photographs of cardiac tissue captured 4 weeks post-MI revealed preservation of LV wall integrity and reduced LV chamber size in FXR^-/- mice (n=7). (B) Triphenyl tetrazolium chloride staining performed on day 28 following MI was used to calculate the infarct/LV area ratio in FXR^-/- and WT mice. (C) Infarct size assessed 4 weeks post-MI was significantly larger in WT compared with FXR^-/- mice (n=4/group). Data are expressed as the mean ± standard error of the mean. *P<0.05 vs. the WT group. MI, myocardial infarction; LV, left ventricle; FXR, farnesoid X receptor; WT, wild type.

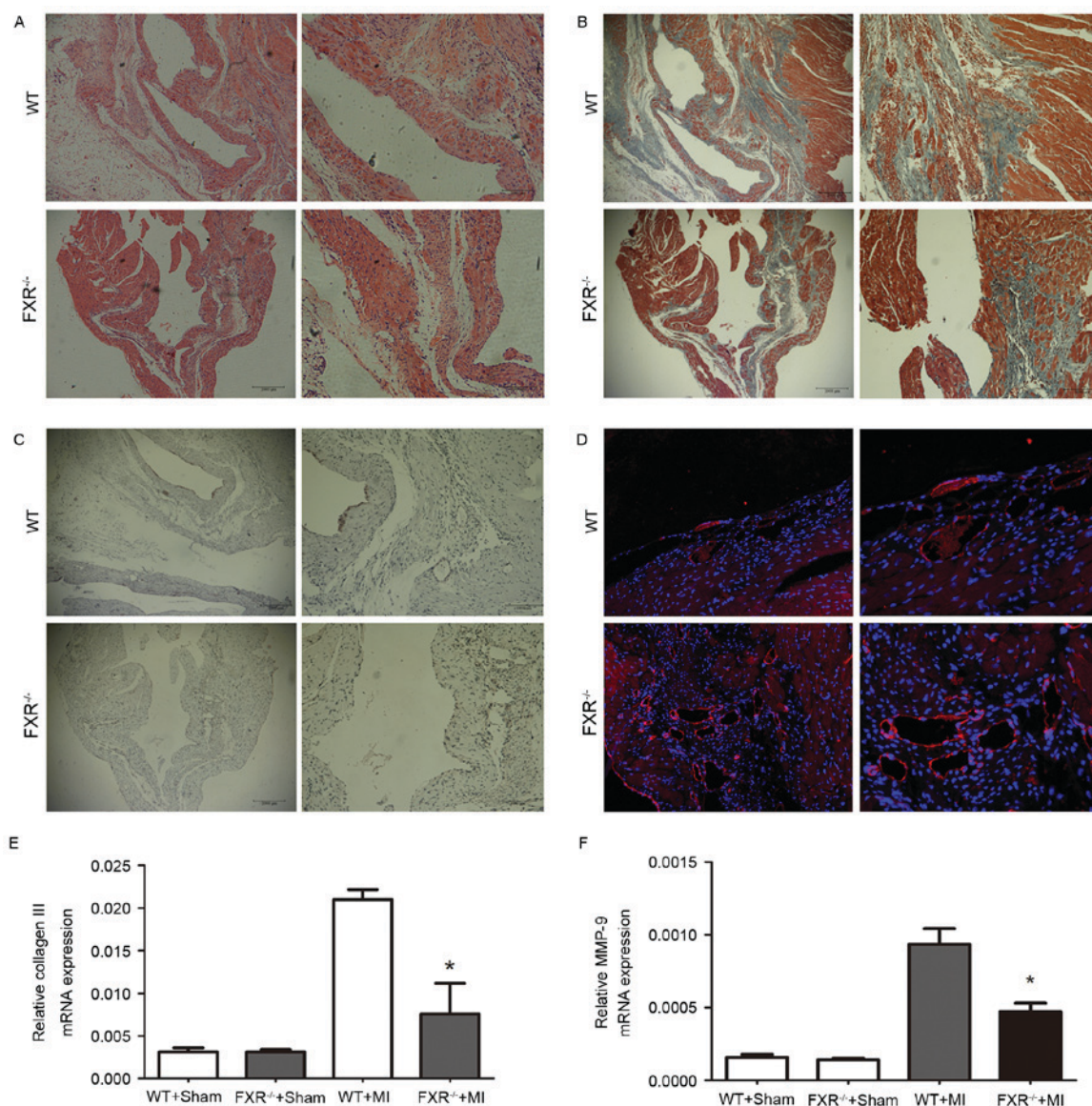demonstrated in Fig. 3B in representative samples from the WT and FXR^-/- groups. The border zone was revealed by

Figure 3. Decreased interstitial fibrosis and increased microvesicular density in the peri-infarct border zone of FXR$^{-/-}$ mice 4 weeks following MI. (A) Representative photomicrographs (x100 and x200 magnification) of serial sections stained with hematoxylin and eosin for the morphological identification of the border zone and infarct areas. (B) Representative photomicrographs (x100 and x200 magnification) of Masson's trichrome-stained sections, captured on week 4 following MI, reveal interstitial fibrosis in the border zone in WT and FXR$^{-/-}$ mice. (C) Representative photomicrographs (x100 and x200 magnification) of sections from the infarcted LV regions of WT and FXR$^{-/-}$ mice stained for α-smooth muscle actin. (D) Representative photomicrographs (x200 and x400 magnification) of cardiac sections from WT and FXR$^{-/-}$ mice stained with anti-cluster of differentiation 31 on day 28 following MI. mRNA expression levels of (E) collagen III and (F) MMP-9 in LV tissue samples were assessed using reverse transcription-quantitative polymerase chain reaction and normalized to GAPDH expression on day 28 following MI. Data are expressed as the mean ± standard error of the mean (n=6 mice/group). *P<0.05 vs. the WT + MI group. FXR, farnesoid X receptor; MI, myocardial infarction; WT, wild type; MMP, matrix metalloproteinase; LV, left ventricular.

H&E staining in serial sections (Fig. 3A). Expression of α-smooth muscle actin (α-SMA) is considered a marker for the conversion of fibroblasts into myofibroblasts in myocardial tissue. FXR$^{-/-}$ mice exhibited a significant reduction in the number of α-SMA positive myofibroblasts in peri-infarct areas compared with WT mice, as assessed on week 4 following MI (Fig. 3C). Microvesicular density was assessed in the border zone using CD31 staining and was revealed to be increased in the FXR$^{-/-}$ compared with in the WT group (Fig. 3D).

The mRNA expression levels of collagen III and MMP-9 were evaluated using RT-qPCR on day 28 following MI. As presented in Fig. 3E and F, collagen III and MMP-9 mRNA levels were upregulated in mice that underwent MI compared with in the sham-operated groups. Furthermore, FXR$^{-/-}$ mice exhibited a marked reduction in collagen III and MMP-9 mRNA levels compared with WT mice 28 days following MI.

Cardiomyocyte apoptosis. Cardiomyocyte apoptosis was assessed using a TUNEL assay. In the border zone, the percentage of TUNEL-positive, i.e., apoptotic, cardiomyocytes was significantly reduced in FXR$^{-/-}$ mice compared with in WT mice (Fig. 4A and B). Western blot analysis revealed a significant reduction in cleaved caspase-3 protein levels in FXR$^{-/-}$ mice compared with in WT mice, as assessed on day 7 post-MI (Fig. 4C and D).
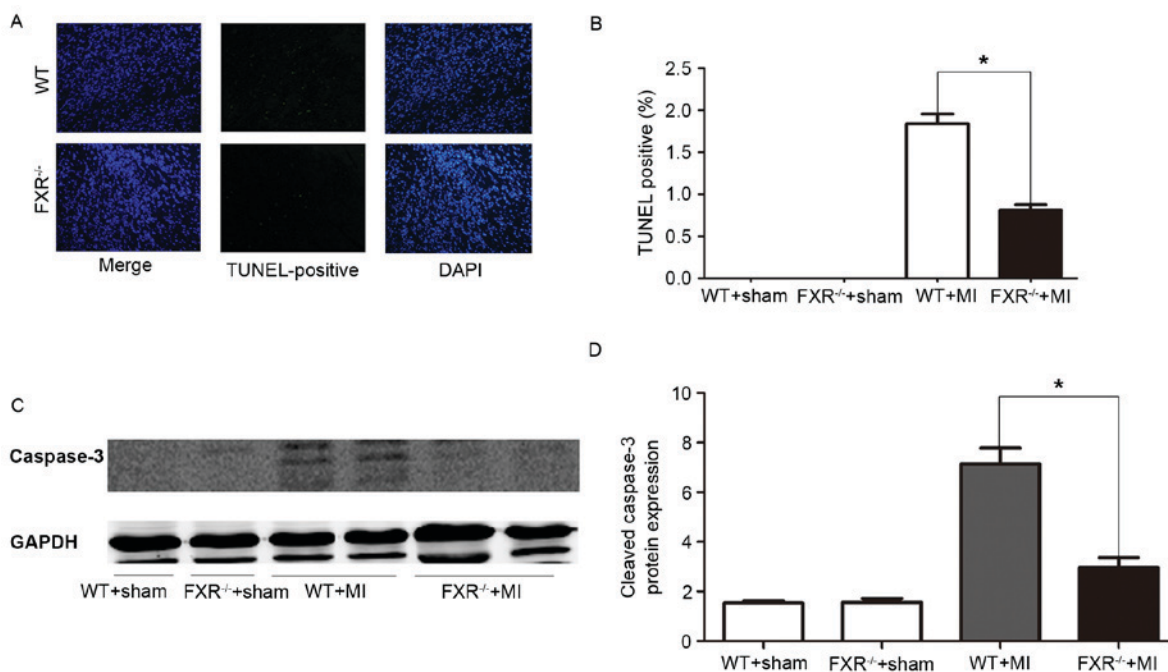
Figure 4. (A) TUNEL assay on day 7 following MI revealed an increase in cardiomyocyte apoptosis in WT vs. FXR^{-/-} mice. Magnification, x200. (B) The ratio of apoptotic/non-apoptotic myocyte was significantly higher in WT mice compared with FXR^{-/-} mice on day 7 following MI (n=3 mice/group, 5 fields/heart). (C) Representative western blot demonstrating cleaved caspase-3 protein expression levels in infarct regions of sham- and MI-operated WT and FXR^{-/-} mice on day 7 following MI. (D) Relative protein expression levels of cleaved caspase-3 were semi-quantified and normalized to GAPDH. Data are expressed as the mean ± standard error of the mean (n=4 mice/group). *P<0.05 vs. the WT + MI group. FXR, farnesoid X receptor; MI, myocardial infarction; TUNEL, terminal deoxynucleotidyl transferase dUTP nick-end labelling; WT, wild type.

Discussion

Patients who recover from MI often develop cardiac fibrosis, which can lead to a decline in cardiac function and ultimately in heart failure (1,24). Cardiac remodeling is a critical process in the development of heart failure following MI (25,26). The mechanisms underlying cardiac remodeling are complex; however, matrix turnover has been reported to serve a central role during the early days and weeks following MI (27,28). It has previously been suggested that the pharmacological inhibition or genetic ablation of FXR may reduce cardiomyocyte apoptosis, decrease infarct size and improve cardiac function in myocardium that has undergone ischemia/reperfusion (13). Therefore, it may be hypothesized that FXR-deficient mice are characterized by deficits in cardiac remodeling and FXR may serve an important role in cardiomyocyte apoptosis following MI. The present results demonstrated an increase in FXR expression in the infarct region that peaked on day 7 and declined at day 28 post-MI. These results suggested that FXR may be implicated in the primary stages of cardiac healing processes that follow MI. To the best of our knowledge, the present study is the first to demonstrate that FXR knockdown attenuated cardiac remodeling following MI. FXR knockdown appeared to reduce infarct size and improve cardiac function following MI, thus suggesting that FXR is implicated in the mechanisms underlying post-MI cardiac remodeling. The observed improvement in post-MI remodeling in FXR-deficient hearts may be attributed to the reduction of cardiomyocyte apoptosis and interstitial fibrosis, and increasing angiogenesis.

It has previously been reported that cardiomyocyte apoptosis is a major mechanism implicated in unfavorable LV remodeling (29). Myocardial cell apoptosis mediated by mitochondria have an important role in the repair of myocardial infarction. FXR activation may lead to significant cardiomyocyte apoptosis and mitochondrial death signaling characterized by caspase-3 activation (13). The present study demonstrated that myocyte apoptosis was suppressed in FXR-deficient mice 7 days post-MI. Additionally, a significant reduction in cleaved caspase-3 protein levels in FXR^{-/-} mice on day 7 post-MI was determined, thus suggesting that the absence of FXR may be associated with the improvement of LV remodeling and cardiac function following MI.

Neoangiogenesis is an essential component of cardiac remodeling processes. Following MI, the existing vasculature is not able to meet the enhanced oxygen demands of the viable myocardium, which may lead to adjacent viable myocardial tissue necrosis, progressive infarct extension and fibrous replacement (25). In the present study, angiogenesis via detection of CD31 appeared to be enhanced in FXR^{-/-} compared with in WT mice, which may contribute to the improvement of cardiac function and LV remodeling following MI.

Previous studies have reported that cardiac extracellular matrix (ECM) dysregulation may participate in progressive LV remodeling, and may lead to excessive collagen deposition, fibrosis and collagen degradation, followed by LV dilatation (27,30,31). Type I and III collagen are among the main components of the ECM, which provides the structure and mechanical support for the heart, and participates in signaling among cardiomyocytes (27). The physiological integrity of the ECM lies under the control of the MMP family of endopeptidases and their specific tissue inhibitors (15). Enhanced expression and activity of MMP-9 has been associated with

collagen formation, whereas MMP-9 deletion has been reported to attenuate myocardial fibrosis (28). The results of the present study revealed that mRNA expression levels of type III collagen and MMP-9 were significantly upregulated in WT compared with FXR$^{-/-}$ mice 4 weeks following MI. It may suggest FXR deletion may reduce the collagen deposition following MI and improve the LV remodeling.

In conclusion, the present results suggested a central role for FXR in myocardial injury and remodeling. To the best of our knowledge, this is the first study to demonstrate the effects of FXR deletion on the preservation of cardiac function following MI and in the suppression of abnormal remodeling. Therefore, FXR may represent a potential novel therapeutic target for the treatment of patients following MI.

References

1. Ma Y, Halade GV, Zhang J, Ramirez TA, Levin D, Voorhees A, Jin YF, Han HC, Manicone AM and Lindsey ML: Matrix metalloproteinase-28 deletion exacerbates cardiac dysfunction and rupture after myocardial infarction in mice by inhibiting M2 macrophage activation. Circ Res 112: 675-688, 2013.
2. Go AS, Mozaffarian D, Roger VL, Benjamin EJ, Berry JD, Blaha MJ, Dai S, Ford ES, Fox CS, Franco S, et al: Heart disease and stroke statistics-2014 update: A report from the American Heart Association. Circulation 129: e28-e292, 2014.
3. Krishnamurthy P, Thal M, Verma S, Hoxha E, Lambers E, Ramirez V, Qin G, Losordo D and Kishore R: Interleukin-10 deficiency impairs bone marrow-derived endothelial progenitor cell survival and function in ischemic myocardium. Circ Res 109: 1280-1289, 2011.
4. Wu S, Yin R, Ernest R, Li Y, Zhelyabovska O, Luo J, Yang Y and Yang Q: Liver X receptors are negative regulators of cardiac hypertrophy via suppressing NF-kappaB signalling. Cardiovasc Res 84: 119-126, 2009.
5. Kuipers I, Li J, Vreeswijk-Baudoin I, Koster J, van der Harst P, Silljé HH, Kuipers F, van Veldhuisen DJ, van Gilst WH and de Boer RA: Activation of liver X receptors with T0901317 attenuates cardiac hypertrophy in vivo. Eur J Heart Fail 12: 1042-1050, 2010.
6. He Q, Pu J, Yuan A, Lau WB, Gao E, Koch WJ, Ma XL and He B: Activation of liver-X-receptor α but not liver-X-receptor β protects against myocardial ischemia/reperfusion injury. Circ Heart Fail 7: 1032-1041, 2014.
7. Lei P, Baysa A, Nebb HI, Valen G, Skomedal T, Osnes JB, Yang Z and Haugen F: Activation of Liver X receptors in the heart leads to accumulation of intracellular lipids and attenuation of ischemia-reperfusion injury. Basic Res Cardiol 108: 323, 2013.
8. Son NH, Yu S, Tuinei J, Arai K, Hamai H, Homma S, Shulman GI, Abel ED and Goldberg IJ: PPARγ-induced cardiolipotoxicity in mice is ameliorated by PPARα deficiency despite increases in fatty acid oxidation. J Clin Invest 120: 3443-3454, 2010.
9. Makishima M, Okamoto AY, Repa JJ, Tu H, Learned RM, Luk A, Hull MV, Lustig KD, Mangelsdorf DJ and Shan B: Identification of a nuclear receptor for bile acids. Science 284: 1362-1365, 1999.
10. Swales KE, Korbonits M, Carpenter R, Walsh DT, Warner TD and Bishop-Bailey D: The farnesoid X receptor is expressed in breast cancer and regulates apoptosis and aromatase expression. Cancer Res 66: 10120-10126, 2006.
11. Parks DJ, Blanchard SG, Bledsoe RK, Chandra G, Consler TG, Kliewer SA, Stimmel JB, Willson TM, Zavacki AM, Moore DD and Lehmann JM: Bile Acids: Natural ligands for an orphan nuclear receptor. Science 284: 1365-1368, 1999.
12. Forman BM, Goode E, Chen J, Oro AE, Bradley DJ, Perlmann T, Noonan DJ, Burka LT, McMorris T, Lamph WW, et al: Identification of a nuclear receptor that is activated by farnesol metabolites. Cell 81: 687-693, 1995.
13. Pu J, Yuan A, Shan P, Gao E, Wang X, Wang Y, Lau WB, Koch W, Ma XL and He B: Cardiomyocyte-expressed farnesoid-X-receptor is a novel apoptosis mediator and contributes to myocardial ischaemia/reperfusion injury. Eur Heart J 34: 1834-1845, 2013.
14. Hageman J, Herrema H, Groen AK and Kuipers F: A role of the bile salt receptor FXR in atherosclerosis. Arterioscler Thromb Vasc Biol 30: 1519-1528, 2010.
15. Bishop-Bailey D, Walsh DT and Warner TD: Expression and activation of the farnesoid X receptor in the vasculature. Proc Natl Acad Sci USA 101: 3668-3673, 2004.
16. Ye L, Jiang Y and Zuo X: Farnesoid-X-receptor expression in monocrotaline-induced pulmonary arterial hypertension and right heart failure. Biochem Biophys Res Commun 467: 164-170, 2015.
17. Gao E, Lei YH, Shang X, Huang ZM, Zuo L, Boucher M, Fan Q, Chuprun JK, Ma XL and Koch WJ: A novel and efficient model of coronary artery ligation and myocardial infarction in the mouse. Circ Res 107: 1445-1453, 2010.
18. Liu X, Gao J, Xia Q, Lu T and Wang F: Increased mortality and aggravation of heart failure in liver X receptor-α knockout mice after myocardial infarction. Heart Vessels 31: 1370-1379, 2016.
19. Pfeffer MA, Pfeffer JM, Fishbein MC, Fletcher PJ, Spadaro J, Kloner RA and Braunwald E: Myocardial infarct size and ventricular function in rats. Circ Res 44: 503-512, 1979.
20. Tang M, Zhong M, Shang Y, Lin H, Deng J, Jiang H, Lu H, Zhang Y and Zhang W: Differential regulation of collagen types I and III expression in cardiac fibroblasts by AGEs through TRB3/MAPK signaling pathway. Cell Mol Life Sci 65: 2924-2932, 2008.
21. Woo YJ, Panlilio CM, Cheng RK, Liao GP, Atluri P, Hsu VM, Cohen JE and Chaudhry HW: Therapeutic delivery of cyclin A2 induces myocardial regeneration and enhances cardiac function in ischemic heart failure. Circulation 114 (1 Suppl): I206-I213, 2006.
22. Livak KJ and Schmittgen TD: Analysis of relative gene expression data using real-time quantitative PCR and the 2(-Delta Delta C(T)) Method. Methods 25: 402-408, 2001.
23. He K, Chen X, Han C, Xu L, Zhang J, Zhang M, Xia Q: Lipopolysaccharide-induced cross-tolerance against renal ischemia-reperfusion injury is mediated by hypoxia-inducible factor-2α-regulated nitric oxide production. Kidney Int 85: 276-288, 2014.
24. Cohn JN, Ferrari R and Sharpe N: Cardiac remodeling-concepts and clinical implications: A consensus paper from an international forum on cardiac remodeling. Behalf of an International Forum on Cardiac Remodeling. J Am Coll Cardiol 35: 569-582, 2000.
25. Ding L, Dong L, Chen X, Zhang L, Xu X, Ferro A and Xu B: Increased expression of integrin-linked kinase attenuates left ventricular remodeling and improves cardiac function after myocardial infarction. Circulation 120: 764-773, 2009.
26. Li Q, Xie J, Li R, Shi J, Sun J, Gu R, Ding L, Wang L and Xu B: Overexpression of microRNA-99a attenuates heart remodelling and improves cardiac performance after myocardial infarction. J Cell Mol Med 18: 919-928, 2014.
27. Bowers SL, Banerjee I and Baudino TA: The extracellular matrix: At the center of it all. J Mol Cell Cardiol 48: 474-482, 2010.
28. Chiao YA, Ramirez TA, Zamilpa R, Okoronkwo SM, Dai Q, Zhang J, Jin YF and Lindsey ML: Matrix metalloproteinase-9 deletion attenuates myocardial fibrosis and diastolic dysfunction in ageing mice. Cardiovasc Res 96: 444-455, 2012.
29. Abbate A, Biondi-Zoccai GG, Bussani R, Dobrina A, Camilot D, Feroce F, Rossiello R, Baldi F, Silvestri F, Biasucci LM and Baldi A: Increased myocardial apoptosis in patients with unfavorable left ventricular remodeling and early symptomatic post-infarction heart failure. J Am Coll Cardiol 41: 753-760, 2003.
30. Souders CA, Bowers SL and Baudino TA: Cardiac fibroblast: The renaissance cell. Circ Res 105: 1164-1176, 2009.
31. Jourdan-Lesaux C, Zhang J and Lindsey ML: Extracellular matrix roles during cardiac repair. Life Sci 87: 391-400, 2010.